UV Near-Resonance Raman Spectroscopic Study of 1,1′-Bi-2-naphthol Solutions

Zun-yun Li, Dong-ming Chen,* Tian-jing He, and Fan-chen Liu*

Department of Chemical Physics, University of Science and Technology of China, Hefei, Anhui 230026, People's Republic of China

Received: January 25, 2007; In Final Form: March 13, 2007

The normal and UV near-resonance Raman (UVRR) spectra of 1,1′-bi-2-naphthol (BN) in basic solution were measured and analyzed. Density functional theory (DFT) calculations were carried out to study the ground state geometry structure, vibrational frequencies ν, off-resonance Raman intensities I, and depolarization ratios ρ of 1,1′-bi-2-naphtholate dianion (BN^{2-}). On the basis of the calculated and experimental results of ν, I, and ρ, the observed Raman bands were assigned in detail. The 1612 cm^{-1} Raman band of BN in basic solution was found dramatically enhanced in the UV resonance Raman spectrum in comparison with the normal Raman spectrum. Analyzing the depolarization ratios of the 1366 and 1612 cm^{-1} bands in the RR spectra manifests that both the symmetric and antisymmetric parts of transition polarizabilities contribute to the 1366 cm^{-1} band, but that only the symmetric part contributes to the 1612 cm^{-1} band.

1. Introduction

Chiral molecules are of great importance in chemical and biochemical areas. Chiral 1,1′-binaphthyl compounds have attracted increasing interests because of their highly stable chiral configuration. They had been extensively utilized as chiral inducers for asymmetric organic synthesis and catalytic reactions.[1,2] Among them, optically active 1,1′-bi-2-naphthol (BN) and its derivatives are extremely useful C_2-symmetric compounds. On one hand, 1,1′-bi-2-naphthol often serves as the starting material to obtain chiral binaphthyl compounds. On the other hand, this special class of compound has been widely used as ligands in chiral metal complexes for asymmetric catalysis and has demonstrated outstanding performance in chiral recognition.[3−6] For example, Ishii et al. investigated asymmetric catalysis of the Friedel−Crafts reaction with fluoral by chiral binaphthol-derived titanium complexes.[5a]

It is known[1] that the outcome of a given asymmetric transformation depends on both steric and electronic properties of the chiral BN ligands. The structures and properties of 1,1′-bi-2-naphthol have been intensively studied with various spectroscopic methods, such as electronic absorption, IR, and Raman spectroscopies. Setnička and co-workers measured the vibrational circular dichroism (VCD) spectra of BN and assigned the observed VCD bands on the basis of density functional theory (DFT) calculations.[7] Sahnoun et al. theoretically studied the mechanism of the isomerization of BN using DFT calculations.[8] Nogueira and co-workers studied the surface-enhanced Raman (SER) spectrum of BN adsorbed on silver colloids for the first time and proposed the empirical assignments for the observed Raman bands.[9] Because BN in various solutions has strong electronic absorption in the near UV region, its UVRR spectra would possibly be detected and could provide more information on both ground and excited states. However, to the best of our knowledge, there is no report on the resonance Raman (RR) spectra of BN in the literature yet.

On the other hand, sum-frequency generation (SFG) of chiral solution as novel spectroscopic tools to probe molecular chirality are currently being developed[10−18] and were reviewed by Belkin and Shen[17a] and Fischer and Hache,[17b] respectively. R(S)-BN solutions as a prototype of chiral compounds have been investigated by various new novel SFG spectroscopies, such as the chiral sum-frequency spectroscopy of electron transitions,[12,15] chiral sum-frequency spectroscopy of vibrational transitions, and doubly resonant SFG (DR-SFG),[14,18] the new chiral electro-optic effect: SFG from optical active BN liquids in the presence of a dc electric field,[16] also second-harmonic generation (SHG) from BN surface,[19] and so on. Resonance Raman spectra of BN solution are closely related to the sum-frequency vibrational spectroscopy (SFVS) investigations of chiral BN solution in many ways. First, the strength of the chiral vibrational peaks in infrared-visible sum-frequency vibrational spectra from isotropic chiral liquids is proportional to the square of the corresponding antisymmetric Raman tensor element,[14] which can be deduced by the Placzek invariants Σ^1 for vibrational peaks in RR spectra.[20] A direct resonance Raman study can provide much-needed experimental data to address the relations between the doubly resonant SFG and the antisymmetric Raman tensors. Second, strong resonance enhancement, detailed assignment of vibration modes, and possible deduction of vibronic coupling for the modes are the advantages of RR spectroscopy, which are useful for the analysis and assignment of the sum-frequency vibrational spectroscopy of the chiral solution.[14,15]

In this paper, we have measured the UV near-resonance Raman spectra of 1,1′-bi-2-naphthol in a basic solution. The resonance enhancement in the intensity, depolarization ratios, and antisymmetric Raman tensors of 1612 and 1366 cm^{-1} vibrational bands in RR spectra have qualitatively been discussed. DFT calculations have been performed to study the ground state structures and vibrational spectra of 1,1′-bi-2-naphthol as well as 1,1′-bi-2-naphtholate dianion (BN^{2-}), because in basic solution, the two hydroxyl groups of BN may undergo deprotonation to form BN^{2-}.[1,6] Empirical and tentative assignments of several vibrational bands in molecular vibrational spectra for BN have briefly and reasonably been analyzed in the literature,[7,9,18] but a complete study on individual assignments for the vibrational spectra of BN and BN^{2-} was not

* Corresponding author. E-mail: dmchen@ustc.edu.cn (D.-M.C.); fcliu@ustc.edu.cn (F.-C.L.).

10.1021/jp070662b CCC: $37.00
Published on Web 05/15/2007

found.[9,14] In this paper, assignments of Raman bands of BN and BN^{2-} have been further proposed and discussed in detail by using the combination of DFT calculation, polarization measurements, and comparison of Raman spectra of BN^{2-} with that of BN.

2. Experimental and Computational Methods

1,1′-Bi-2-naphthol was purchased from Alfa Aesar and was used without further purification. The BN^{2-} and BN solutions were prepared by dissolving BN in 3 M NaOH aqueous and acetone solvents, respectively, with the concentration ranging from 0.3 to 0.05 M. The prepared solutions were allowed to equilibrate for 3 days before spectral measurements.

UV−vis absorption spectra were measured with a 5 mm light-path quartz cell at room temperature using a Shimadu UV-2401PC spectrometer. Raman spectra were recorded on a Jobin-Yvon LABRAM-HR 800 spectrometer equipped with an air-cooled CCD detector, a notch filter, and a 600 grooves/mm grating for the visible and a 2400 grooves/mm UV grating. A lens with 40 mm focal length was used to focus the incident laser beam and collect the scattering light with a back-scattering geometry. The 325 nm line of a He−Cd laser and the 514.5 nm line of an Ar ion laser were used as the excitation sources with the power 3.5 mW and 1 mW, respectively, on the sample. The collection time of the CCD detector was 80−180 s for Raman spectra. To minimize any damage of the sample due to the prolonged exposure to laser radiation, we recorded UV resonance Raman spectrum of solutions using a rotating cell. Depolarization ratios of Raman bands were measured under the same conditions. The parallel and perpendicular components of the polarized Raman spectra of solution samples were obtained with a polarizer oriented parallel and perpendicular, respectively, to the polarization direction of the incident laser beam. As the spectrometer is not equipped with the polarization scrambler to avoid polarization detection biases, the polarized Raman scattering of tetrachloromethane and cyclohexane were measured to check and calibrate the depolarization ratios of the studied species.

DFT calculations of BN and BN^{2-} molecules were carried out using Becke et al.'s three-parameter hybrid functional (referred as B3LYP),[21] which has been suitable for studying the structures and properties of BN systems.[8,18] To reduce computational cost, we carried out the initial searching of steady structure of the studied molecule by geometry optimization with relatively small basis sets, 6-31G, without any symmetry constraint. The obtained structures were then used for the final optimization using 6-31G* basis sets with suitable symmetry (C_2 point group) constraint. Analytic frequency calculations (using B3LYP/6-31G*) at the optimized structure were done to confirm the optimized structures to be an energy minimum and to obtain the theoretical vibrational spectra. Because of the neglect of the anharmonicity and the incomplete basis sets, the DFT calculations tend to slightly overestimate the vibrational frequencies. The systematic discrepancies between the computed and experimental frequencies can be corrected by scaling the calculated frequencies with a single factor.[23] Oakes et al. suggested that a standard value of 0.98 is appropriate for the planar conjugate systems such as the porphyrins.[23] This factor is used in the present study. Assignment of individual vibrational frequency was carried out by inspecting the calculated Cartesian displacements of the corresponding normal mode. All calculations were performed with the Gaussian 03 program suite[26] on a P4-3.0G computer.

In this paper, we use isolated single molecule computations to predict solution-phase geometry and vibrational frequencies.

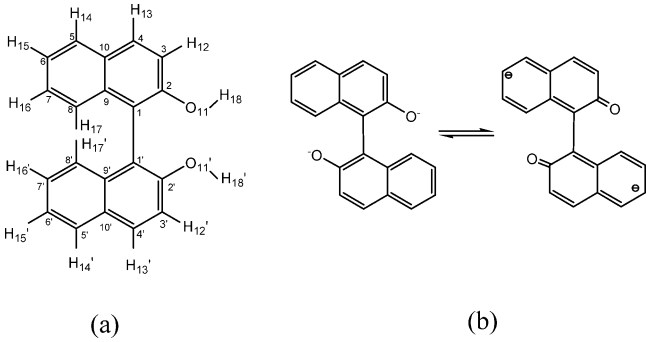

Figure 1. (a) Structural sketch of BN with the labels of the atoms. (b) Resonance structures of the BN^{2-} dianion.

There may be errors associated with it and the differences may be significant for a dianion particularly. But at present, the practice is common in most of the literature of quantum chemistry computations. For examples, by similar strategy Markham et al. successfully developed ab initio computation treatment of the effect of deuterium substitution on resonance Raman spectra of imidazole, imidazolium, and their derivatives,[22] where the solvent effect are large and probably more so than in this study. Pasterny et al.'s theoretical calculations indicated that there is no significant change in calculated vibrational frequencies as a function of medium polarity.[24]

3. Results and Discussion

3.1. Ground-State Geometries and Atomic Charges. DFT calculations were carried out to study the ground-state geometry structure of BN^{2-}. The calculated results indicate that BN^{2-} has a *trans*-quinonoid-like structure, as shown in Figure 1b, which agrees with the experimental results of BN in basic solution.[1,6] Table 1 lists the bond lengths, bond angles, and dihedral angles of BN^{2-} optimized with B3LYP/6-31G*. For the sake of comparison, the structure of BN was also calculated with the same theoretical level, and the results were listed in Table 1 together with the X-ray crystallographic results.[27] Figure 1a shows the structural sketch and atomic labels of BN used in this paper.

It can be seen from Table 1 that the computed bond lengths and angles of BN are generally in agreement with the experimental values.[27] B3LYP/6-31G* calculations indicate that the two naphthol rings of BN molecule are almost perpendicular with each other. The dihedral angle ($C_2-C_1-C_{1'}-C_{9'}$) between the planes of the naphthyl groups is 92.7°, which is consistent with the corresponding X-ray value (99.2°) of BN.[27] Deprotonation of the hydroxyl groups leads to the two naphthyl groups being twisted toward a more coplanar orientation, giving rise to a more acute dihedral angle (68.3°). DFT calculation of BN^{2-} reveals evident changes on the C−O bond and the C−C bond adjacent to the hydroxyl groups. Compared with BN, the C_1-C_2, C_2-C_3, and C_9-C_{10} distances of BN^{2-} are calculated to increase by 0.067, 0.049, and 0.017 Å, respectively, whereas the C_1-C_9 distance is found to decrease by 0.013 Å. Particularly, the C−O bond length of BN^{2-} decreases by 0.105 Å in comparison with that of BN. The calculation results of the bond lengths and dihedral angles indicate that BN^{2-} has a quinonoid-like structure shown in Figure 1b.

Natural population analyses (NPA) are performed with B3LYP/6-31G(d) for the ground-states of BN and BN^{2-}. Table 2 gives the charge distribution on the oxygen atoms and the ring carbon atoms for both BN and BN^{2-}. It can be seen that most of the carbon atoms are negatively charged, except C_2, which bears a positive charge. The NPA calculations reveal a

TABLE 1: Calculated Structural Parameters of BN and BN^{2-} and Experimental Values of BN

	BN^{2-} (calcd)[a]	BN (calcd)[a]	BN (exp)[b]
	bond distances (Å)		
C_1-C_2	1.454	1.387	1.382
C_2-C_3	1.467	1.418	1.410
C_3-C_4	1.367	1.373	1.351
C_4-C_{10}	1.423	1.418	1.418
C_5-C_{10}	1.414	1.420	1.426
C_5-C_6	1.383	1.376	1.353
C_6-C_7	1.420	1.416	1.393
C_7-C_8	1.377	1.377	1.369
C_8-C_9	1.437	1.423	1.411
C_9-C_{10}	1.452	1.435	1.423
C_9-C_1	1.417	1.430	1.424
C_2-O_{11}	1.263	1.368	1.370
$C_1-C_{1'}$	1.498	1.495	1.494
	bond angles (deg)		
$C_1-C_2-C_3$	115.4	121.3	121.1
$C_2-C_3-C_4$	124.0	120.4	120.2
$C_3-C_4-C_{10}$	120.8	120.8	121.6
$C_{10}-C_5-C_6$	122.1	121.0	121.0
$C_5-C_6-C_7$	118.3	119.7	120.5
$C_6-C_7-C_8$	121.2	120.8	120.3
$C_7-C_8-C_9$	122.5	121.1	121.6
$C_8-C_9-C_1$	122.6	122.1	122.4
$C_1-C_9-C_{10}$	121.8	119.9	119.7
$C_2-C_1-C_9$	120.2	118.8	119.1
	dihedral angles (deg)		
$C_2-C_1-C_{1'}-C_{2'}$	111.1	86.5	
$C_2-C_1-C_{1'}-C_{9'}$	68.3	92.7	99.2

[a] DFT calculations using 6-31G* basis-sets. [b] X-ray results from ref 27.

TABLE 2: Calculated NPA Charges for BN and BN^{2-}

	BN	BN^{2-}
C1	−0.089	−0.145
C2	0.350	0.406
C3	−0.298	−0.298
C4	−0.190	−0.250
C5	−0.204	−0.229
C6	−0.245	−0.323
C7	−0.228	−0.274
C8	−0.214	−0.211
C9	−0.023	−0.028
C10	−0.074	−0.107
O11	−0.680	−0.731

positive charge (0.196 e) on the naphthalene ring in BN, whereas there is a negative charge (−0.269 e) on the naphthalene ring of BN^{2-}, reflecting an averaged population of exceed electrons on the oxygen atom and the naphthalene rings of BN^{2-}. Charge redistribution has been analyzed by comparing the electron densities of the BN^{2-} with those of BN. Upon deprotonation of the hydroxyl, the electron populations are increased for most carbon atoms on the naphthalene ring. For the BN^{2-}, the excess negative charges are found populated mainly on the C_1, C_7, C_{10}, and particularly the C_6 atoms, in comparison with the BN molecule. This is in agreement with the resonance structure shown in Figure 1b.

3.2. UV−Visible Absorption Spectra. Figure 2 displays the UV−vis absorption spectra of 1,1′-bi-2-naphthol dissolved in a 3 M NaOH aqueous solution and in acetone, respectively. In acetone, the spectrum has two peaks, with the absorption maximums at 324 and 336 nm. For BN in the basic solution, the absorption peak shifts to 358 nm with an asymmetrically broadened shape.

The excitonic splitting should be different for BN and BN^{2-}, as the dihedral angle in the anion is no longer close to 90° and can induce relatively larger splitting. This may be one of relevant reasons why BN^{2-} shows a larger peak width. Another important factor for peak width is due to the Franck−Condon progression in the absorption spectra. The most striking evidence for the Franck−Condon progression nature of the doublet, which was demonstrated by Fischer et al.,[15] is that the electronic spectrum of BN indeed resembles that of 2-naphthol (2HN), and 2HN itself already exhibits a doublet. In addition, the solvent effect is also important for broadening the shape. The red-shift of the UV absorption of BN in the basic solution as compared with that in acetone can be attributed to the enhanced electronic conjugation on the excited-states of BN^{2-}, which were well-recognized for the conjugate anionic bases of hydroxyaryls.[28,29]

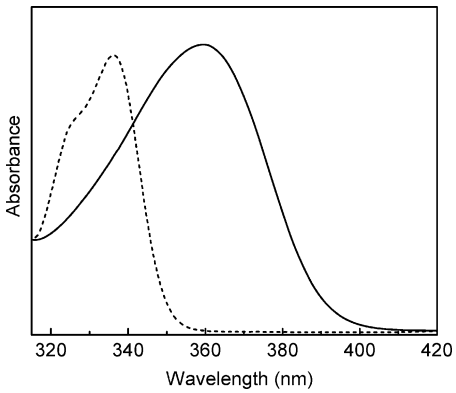

Figure 2. UV−visible absorption spectra of BN in a 3 M NaOH aqueous solution (solid line) and in an acetone solution (dot line).

3.3. Raman Spectra. BN^{2-} dianion has 34 atoms and 96 modes of vibration, which, according to the C_2 symmetry, can be classified as $\Gamma = 49A + 47B$. The vibrations of BN molecule, which have two additional hydrogen atoms, can be classified as $\Gamma = 52A + 50B$. According to the vibrational selection rules, all of these modes are active for both IR and Raman transitions. For normal nonresonance Raman, depolarization ratios usually have a value between 0 and 0.75. The depolarization ratio is less than 0.75 for a totally symmetric mode, whereas it equals 0.75 for a nontotally symmetric mode. As such, polarized Raman measurements can be used to determine the symmetry of a specific mode.

Nogueira et al. studied the SERS of BN with 1064 nm excitation and proposed tentative assignments for several strong Raman bands.[9] In this paper, the UV resonance Raman spectra and normal Raman spectra of BN in the basic solution were recorded. More complete assignments and some reassignments of Raman bands have been made on the basis of DFT calculations, polarization measurements, and comparison of Raman spectra of BN^{2-} with that of BN. Figure 3 displays the normal Raman spectra of BN in an acetone solution or as solid powder with 514.5 nm excitation, normal ($\lambda_{ex} = 514.5$ nm) and near-resonance ($\lambda_{ex} = 325$ nm) Raman scattering of BN in aqueous NaOH solution, where the Raman signals due to the solvent (acetone) are marked as "S". Tables 3 and 4 list the experimentally observed and DFT-calculated frequencies, intensities, depolarization ratios, and assignments of Raman bands of BN and BN^{2-}. The assignments will be discussed in detail in the following section 3.3.1. Because of the steric hindrance of OH group and hydrogen bonding in BN solutions,[7] we consider BN and BN^{2-} as rigid molecules and do not make the average for the dihedral angle between two aromatic planes for dependent properties. Although a similar strategy was used in some related references,[7,18] further detailed investigations are needed. A recent work relating to this has been conducted by Devlin et al., who carefully investigated configurational and

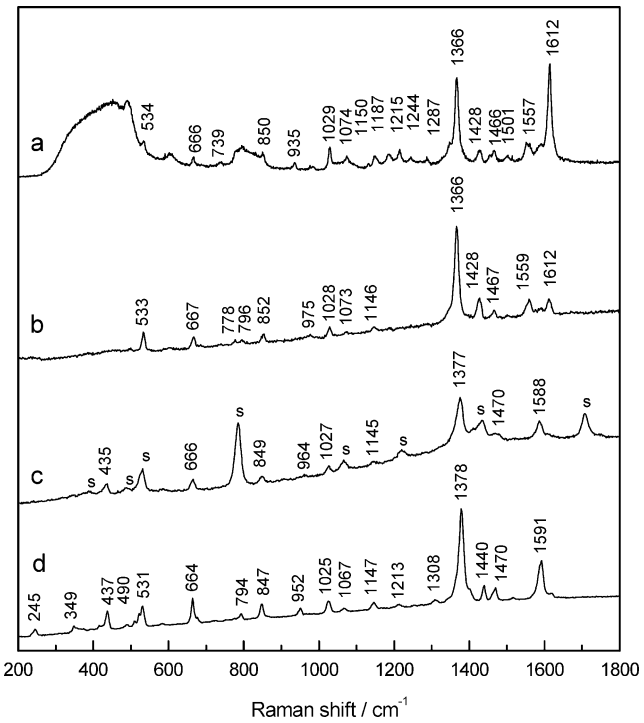

Figure 3. Raman spectrum of BN (a) in a 3 M NaOH aqueous solution, λ_{ex}= 325 nm; (b) in a 3 M NaOH aqueous solution, λ_{ex}= 514.5 nm; (c) in an acetone solution, λ_{ex}= 514.5 nm; (d) as a solid powder, λ_{ex}= 514.5 nm.

conformational analysis of some chiral molecules using IR and VCD spectroscopies and ab initio density functional theory.[25]

3.3.1. Raman Spectra Excited at 514.5 nm. Figure 4 presents the polarized Raman spectra of BN in a 3 M NaOH aqueous solution and in acetone excited at 514.5 nm. Figure 5 shows the Cartesian displacements of some strong Raman bands of BN^{2-} calculated with B3LYP/6-31G*. In the Raman spectrum of BN^{2-} (Figure 4b), strong Raman bands were observed at 533, 667, 852, 975, 1028, 1366, 1428, 1467, 1559, 1592, and 1612 cm^{-1}. These bands are considered corresponding to the totally symmetric vibrations because their depolarization ratios are less than 0.75. The strongest band of BN^{2-} was observed at 1366 cm^{-1}, which apparently corresponds to the 1377 cm^{-1} band of BN in acetone solution (Figure 4a) in light of their similar intensities and depolarization ratios. In the 1064 nm excited SERS of BN, this band was also observed with considerable intensity and was assigned to the C−O stretching mode.[9] However, our DFT calculation does not find a suitable candidate for the C−O stretching mode in the region. In contrast, B3LYP/6-31G* calculation of BN^{2-} predicts a very strong Raman at 1357 cm^{-1} due to the C_9C_{10}/C_9C_1 stretching mode (corresponding to the ν_5 mode of naphthalene, according to Scherer[30]). We thus assign the observed 1366 cm^{-1} band of BN^{2-} to the C_9C_{10}/C_9C_1 stretching vibration with A symmetry. For the neutral BN molecule, the corresponding mode was calculated at 1387 cm^{-1} with a remarkable Raman intensity, which is close to the measured value (1377 cm^{-1}). The B3LYP/6-31G* calculation of BN indicates that, although this mode is mainly due to the stretches of C_9C_{10}/C_9C_1 bonds, the $O_{11}-H_{18}$ in-plane bending is also involved in this mode. Therefore, it is expected that the deprotonation of the −OH groups will cause an evident effect on its frequency. DFT computation predicts a large downshift by 30 cm^{-1} for this mode upon deprotonation. Experimentally, an 11 cm^{-1} downshift was observed for the 1366 cm^{-1} band of BN^{2-} as compared with BN, which is smaller than the computed value but nevertheless is qualitatively coincident with the theoretical prediction.

In the 1550−1650 cm^{-1} region, three polarized Raman bands were observed at 1559, 1592, and 1612 cm^{-1}, respectively, for the BN^{2-} dianion. The 1559 and 1612 cm^{-1} bands of BN^{2-} are much stronger than the 1592 cm^{-1} band. Nogueira et al. have empirically assigned these bands to the C−C stretching of naphthyl rings.[9] Our DFT calculation for BN^{2-} dianion indicates that, although the weak 1592 cm^{-1} band can be attributed to the stretching of $C_7C_8/C_3C_4/C_{10}C_5$ bonds of the naphthyl rings, the strong 1559 and 1612 cm^{-1} bands involve both the C_2O_{11} stretching and the naphthyl C_3C_4/C_5C_6 stretching. For the BN solid, a strong band at 1591 cm^{-1} and a weak band at 1619 cm^{-1} were observed in this region. We attribute them to the calculated vibrations at 1606 and 1630 cm^{-1}. The B3LYP/6-31G* calculation manifests that these two modes are associated mainly with the naphthyl CC stretching and the $O_{11}H_{18}$ bending, and the 1630 cm^{-1} mode also contains a significant contribution from C_2O_{11} stretching. As both of them involve the vibrations of −OH groups, the deprotonation of the −OH groups is expected to induce significant frequency shifts for these two modes. This seems to account for the evident difference for the Raman spectra of BN and BN^{2-} in the 1550−1650 cm^{-1} region.

Most of the vibrations of BN and BN^{2-} in the 900−1500 cm^{-1} region are due to the naphthyl in-plane CC stretching and CH bending. Two strong Raman bands were observed at 1467 and 1428 cm^{-1} for BN^{2-} (Figure 3b). The corresponding bands were observed at 1470 and 1440 cm^{-1} for the BN solid (for BN in acetone solution, the 1440 cm^{-1} band is overlapped with a solvent band). On the basis of our DFT calculations, these two bands are assigned to the naphthyl CC stretching that are coupled to the C−H in-plane bending, corresponding to the ν_{29} and ν_4 modes of naphthalene (according to Scherer's notation[30]). DFT calculations predict 1 cm^{-1} and 35 cm^{-1} downshifts, respectively, for these two modes of BN^{2-} as compared with the BN. Experimentally, we observed a 3 cm^{-1} downshift for the 1467 cm^{-1} band and a 12 cm^{-1} downshift for the 1428 cm^{-1} band of BN^{2-}, as compared with their counterparts of BN, is qualitatively coincident with the calculations.

We assign the observed Raman bands of BN^{2-} at 1146, 1028, and 975 cm^{-1} to the in-plane vibrations of naphthyl groups, corresponding to Scherer's ν_6 (in-plane bending of C_6H/C_7H), ν_{24} (the stretch of C_6C_7 bond), and ν_{32} (in-plane deformation of naphthyl ring). The B3LYP/6-31G* calculated frequencies for these modes were at 1143, 1024, and 975 cm^{-1}, respectively. For the BN molecule, the corresponding bands were observed at 1145, 1027, and 964 cm^{-1} and were calculated at 1158, 1037, and 957 cm^{-1}. The similarity in frequencies and intensities for these bands in BN and BN^{2-} indicate that the deprotonation of −OH groups induce a relative small effect on the CH and CC stretch of distal benzoring, whereas it induces a moderate effect the in-plane deformation of naphthyl ring.

Our DFT calculations manifest that the vibration of BN and BN^{2-} in the 700−850 cm^{-1} region are mainly due to the in-plane deformations of naphthyl ring. We assign the observed 852 cm^{-1} band of BN^{2-} and the 849 cm^{-1} band of BN to the deformations of distal benzo ring (Scherer's ν_{16} mode, which is largely due to the out-of-phase expansion of the $C_3C_4C_{10}$ and $C_6C_7C_8$ bond angles). DFT calculations predict this band to appear at 835 and 848 cm^{-1} for BN^{2-} and BN, respectively, with moderately strong Raman intensities. Although the DFT calculated frequency is consistent with the observed value of BN, the frequency of this mode in BN^{2-} seemed underestimated by DFT calculations.

TABLE 3: Calculated and Observed Frequencies (ν, in cm^{-1}), Raman Intensities (I), and Depolarization Ratios (ρ) of BN

	calcd			obsd			
symmetry	ν^a	I^a	ρ^a	ν^b	ν^c	ρ^c	assignment[d]
B	1630	1.3	0.75	1619			νC_1-C_2, νC_2-O_{11}, νC_3-C_4, νC_5-C_6, νC_7-C_8, $\delta O-H$
A	1606	211	0.48	1591	1588	0.47	$\nu C_1-C_{1'}$, νC_2-C_3, νC_6-C_7, νC_9-C_{10}, $\delta O-H$
A	1498	38	0.05	1517			ν C_2-O_{11}, δC_3-H, δC_7-H
A	1454	48	0.37	1470	1470	~0.20	νC_7-C_8, νC_1-C_9, $\nu C_{10}-C_5$
B	1451	34	0.75	1440			νC_7-C_8, νC_1-C_9, $\nu C_{10}-C_5$
A	1387	199	0.03	1378	1377	0.15	νC_9-C_{10}, $\delta O-H$, ν C_2-O_{11}
A	1305	40	0.01	1308			$\nu C_1-C_{1'}$, $\delta O_{11}-H$
A	1287	5.5	0.745	1274	1282	~0.40	$\nu C-O$, νC_8-C_9, δC_5-H, δC_7-H, δC_8-H
B	1254	2.3	0.75	1255			δC_5-H, δC_8-H
B	1214	5.6	0.75	1213			$\delta O_{11}-H$
A	1158	12	0.69	1147	1145	~0.50	δC_6-H, δC_5-H, δC_4-H, δC_7-H
A	1076	7.4	0.02	1067	1067		$\nu C_1-C_{1'}$, $\delta C_7-C_8-C_9$, $\delta C_{10}-C_5-C_6$, δC_4-H
A	1037	24	0.04	1025	1027	0.17	νC_6-C_7, $\delta C_6-C_7-C_8$, $\delta C_5-C_6-C_7$, δC_5-H, δC_6-H, δC_7-H, δC_8-H
A	957	9.1	0.18	952	964	0.11	$\delta C_1-C_2-C_3$, $\delta C_{10}-C_5-C_6$, $\delta C_6-C_7-C_8$, $\delta C_8-C_9-C_{10}$
A	848	23	0.05	847	849	0.05	$\delta C_3-C_4-C_{10}$, $\delta C_6-C_7-C_8$
B	790	12	0.75	794			γC_8-H, γC_3-H, γC_4-H, γC_5-H
A	668	27	0.07	664	666	0.06	$\delta C_7-C_8-C_9$, $\delta C_{10}-C_5-C_6$
A	581	5.2	0.13	582	584	0.10	τC_1, τC_2, τC_4, τC_{10}, τC_3, γC_3-H, γC_4-H, γC_6-H, γC_8-H, γC_5-H
A	533	12	0.12	531	531		$\delta C_6-C_7-C_8$, $\delta C_9-C_{10}-C_5$, $\delta C_2-C_3-C_4$
B	523	9.4	0.75	522			$\delta C_6-C_7-C_8$, $\delta C_9-C_{10}-C_5$, $\delta C_2-C_3-C_4$
A	508	5.4	0.16	509			τC_9, τC_{10}, τC_1, τC_4, γC_4-H, γC_5-H, γC_8-H, $\delta O_{11}H$
B	485	3.5	0.75	490			τC_9, τC_{10}, τC_5, τC_8, γC_5-H, γC_8-H, γC_4-H
A	434	10	0.10	437	435	0.32	τC_9, τC_{10}, τC_5, τC_8, γC_5-H, γC_8-H
A	423	5.0	0.57	416			τC_5, τC_8, τC_3, γC_5-H, γC_8-H, γC_3-H
A	364	3.4	0.71	374			τC_4, τC_1, τC_2, τC_3, τC_9, γC_4-H, γC_7-H, $\gamma O_{11}H$
A	346	4.3	0.64	349			$\gamma O-H$
A	232	1.5	0.66	245			τ_{butt}

[a] Calculated with B3LYP/6-31G*; frequency scaling factor = 0.98. [b] From solid Raman spectra excited at 514.5 nm. [c] From solution Raman spectra (in acetone) excited at 514.5 nm. [d] Mode assignments: ν, bond stretching; δ, in-plane (naphthyl) bond bending; γ, out-of-plane (naphthyl) wagging of hydrogen atoms; τ, out-of-plane (naphthyl) torsion of carbon atoms; τ_{butt}, butterly torsion between two naphthyl rings.

TABLE 4: Calculated and Observed Frequencies (ν, in cm^{-1}), Raman Intensities (I), and Depolarization Ratios (ρ) of BN^{2-}

	calcd			obsd			
symmetry	ν^a	I^a	ρ^a	ν^b	ν^c	ρ^b	assignment[d]
A	1623	57	0.14	1612	1612	0.57	νC_2-O_{11}, νC_3-C_4, νC_5-C_6, νC_7-C_8
A	1611	181	0.70	1592	1590	0.55	νC_7-C_8, νC_3-C_4, $\nu C_{10}-C_5$
A	1558	90	0.34	1559	1557	0.37	ν C_2-O_{11}, νC_5-C_6, νC_3-C_4
A	1525	27	0.43	1549		0.52	νC_6-C_7, νC_4-C_{10}, δC_7-H
A	1500	163	0.18		1502		νC_8-C_9, $\nu C_{10}-C_5$, δC_8-H, δC_5-H,
A	1453	102	0.63	1467	1466	0.34	νC_1-C_9, νC_3-C_4, δC_6-H, δC_7-H, δC_8-H
B	1444	9.0	0.75		1455		νC_1-C_9, νC_3-C_4, δC_6-H, δC_7-H, δC_8-H
A	1416	117	0.71	1428	1428	0.40	νC_2-C_3, νC_3-C_4, νC_5-C_6, δC_3-H, δC_4-H
A	1357	135	0.14	1366	1366	0.15	νC_9-C_{10}, νC_1-C_9, νC_5-C_{10}
A	1297	96	0.08		1287		$\nu C_1-C_{1'}$, νC_1-C_2
A	1234	69	0.23		1244		νC_1-C_2, $\nu C_{10}-C_5$, δC_5-H, δC_8-H
A	1218	26	0.47		1215		$\nu C_{10}-C_4$, νC_8-C_9, δC_4-H, δC_8-H
A	1156	12	0.48		1187		$\nu C_1-C_{1'}$, δC_3-H, δC_7-H
A	1143	30	0.69	1146	1150	~0.50	δC_6-H, δC_7-H
A	1128	11	0.27		1132		δC_3-H, δC_6-H, δC_7-H
A	1049	51	0.16	1073	1074	~0.25	$\nu C_1-C_{1'}$, δC_4-H, $\delta C_2-C_3-C_4$
A	1024	48	0.26	1028	1029	0.18	νC_6-C_7, $\delta C_6-C_7-C_8$, $\delta C_5-C_6-C_7$, δC_5-H, δC_6-H, δC_7-H
A	975	5.4	0.09	975	980	0.30	$\delta C_8-C_9-C_{10}$, $\delta C_6-C_7-C_8$, $\delta C_{1'}-C_1-C_2$
B	949	0.8	0.75		935		$\delta C_1-C_2-C_3$, δC_4-H
A	835	25	0.05	852	850	0.06	$\delta C_3-C_4-C_{10}$, $\delta C_6-C_7-C_8$, $\delta C_5-C_6-C_7$
B	805	2.6	0.75	796		0.75	γC_7-H, γC_4-H, γC_3-H, τC_9, τC_2
B	760	14	0.75	778		0.75	νC_9-C_{10}, γC_7-H, γC_8-H, γC_3-H, γC_4-H
A	730	9.2	0.73	737	739	~0.67	$\delta C_2-C_3-C_4$, $\delta C_5-C_6-C_7$
A	659	41	0.18	667	666	0.19	τC_2, τC_6, γC_3-H, γC_4-H, γC_8-H
A	522	32	0.10	533	534	0.16	$\delta C_6-C_7-C_8$, $\delta C_9-C_{10}-C_5$, $\delta C_2-C_3-C_4$

[a] Calculated with B3LYP/6-31G*; frequency scaling factor = 0.98. [b] From solution Raman spectrum (in 3 M NaOH) excited at 514.5 nm. [c] From solution Raman spectra (in 3 M NaOH) excited at 325 nm. [d] Mode assignments: ν, bond stretching; δ, in-plane (naphthyl) bond bending; γ, out-of-plane (naphthyl) wagging of hydrogen atoms; τ, out-of-plane (naphthyl) torsion of carbon atoms.

The two weak Raman bands at 796 and 778 cm^{-1} of BN^{2-} have the depolarization ratios about 0.75 and are thus considered as belonging to the asymmetry vibrations. On the basis of the match of calculated and observed frequencies and depolarization ratios, we tentatively assign these two bands to the calculated vibrations of BN^{2-} at 805 and 760 cm^{-1}. According to the DFT calculations, the vibration calculated at 760 cm^{-1} is due to the in-plane breathing mode of naphthyl ring (Scherer's ν_8 mode for naphthalene), whereas the one at 805 cm^{-1} is attributed to the C−H out-of-plane wagging mode of naphthyl ring.

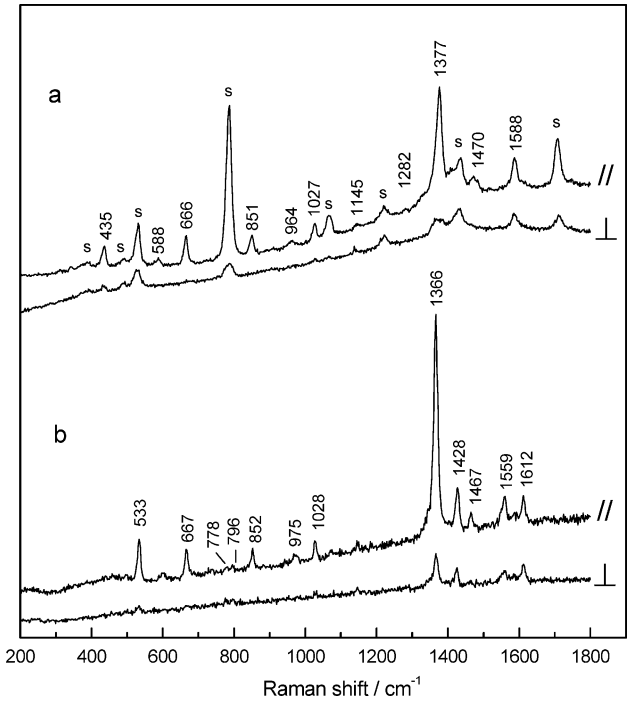

Figure 4. Polarized Raman spectra of BN (a) in an acetone solution; (b) in a 3 M NaOH solution with the excitation wavelength λ_{ex}= 514.5 nm.

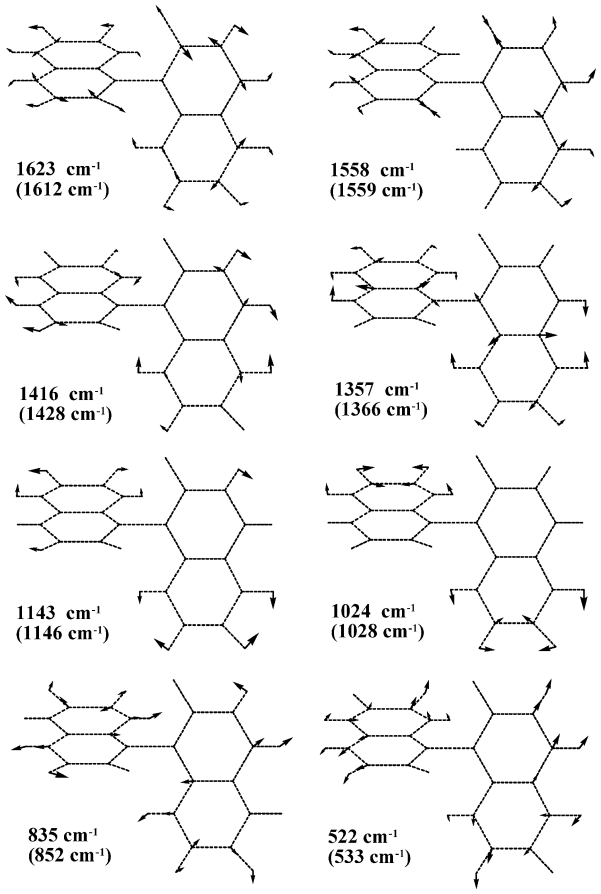

Figure 5. Schematic diagram showing the Cartesian displacements of selected Raman active modes of BN^{2-} calculated with B3LYP/6-31G*. The calculated (plain text) and the measured (in parenthesis) frequencies have been shown for each mode.

DFT calculation for BN^{2-} predicts a strong Raman band at 659 cm^{-1} with A symmetry. We assign the strong band of BN^{2-} at 667 cm^{-1} to this mode. The calculated Cartesian atomic displacements of this mode suggest it to be the C−H out-of-plane wagging. The observed depolarization ratio (0.19) of this mode is consistent with the calculated value (0.18). Its counterpart in BN was observed at 666 cm^{-1}, which is consistent with the DFT calculation.

In the low-frequency region, a strong Raman band was observed at 533 cm^{-1} for BN^{2-} (in a 3 M NaOH solution) and at 531 cm^{-1} for the BN solid. In the Raman spectrum of BN in an acetone solution, this band is overlapped with a Raman band of acetone. We assign it to the in-plane naphthyl deformation (Scherer's ν_{33} mode for naphthalene) that was calculated at 522 cm^{-1} for BN^{2-} and 533 cm^{-1} for BN. The experimental value depolarization ratio of this mode in BN^{2-} is 0.16, consistent with the calculated value (0.10).

A Raman band at 435 cm^{-1} was observed for BN in the solid state and in an acetone solution. This band completely disappeared in BN^{2-}. We tentatively assign it to an O−H out-of-plane rocking vibration. DFT calculations predict a rather lowered frequency for the O−H out-of-plane rocking vibration (at 346 cm^{-1}). The difference between calculation and experiments is thought to be due to the overlook of the hydrogen-bonding interaction in the calculating model,[31] which is expected to have a significant effect on the O−H out-of-plane rocking modes of BN molecule.

In the forgoing analyses, DFT computation has made semiquantitative predictions of the frequency shift of the vibrational bands due to the deprotonation of hydroxyls in BN. The deprotonation also has evident effects on intensities, depolarization ratios, and other properties of Raman bands (see Figures 3 and 4). This has not been considered in this paper and needs to be further investigated because the deprotonation phenomena are significant in solutions.[22]

3.3.2. UV Near-Resonance Raman Spectra (UVRRS) Excited at 325 nm. In the 325 nm excited resonance Raman spectrum of BN in basic solution, several features were observed in the 900−1620 cm^{-1} region (Figure 3a). As shown in Figure 3a, the Raman band of BN in basic solution at 1612 cm^{-1} display great enhancement, which is even stronger than the band at 1366 cm^{-1}. This great resonance enhancement may result from the approximate double resonance in Raman scattering and the Tsuboi's rule of near-resonance enhancement, which are discussed as follows.

First, it is known[32] that the double resonance is defined as enhancement in the intensity of the scattered photon emission under conditions where (i) the energies, $\hbar\omega_1$ and $\hbar\omega_2$, of the incident and scattering photons coincide with those of two excitation energy levels and (ii) the difference $\hbar(\omega_1 - \omega_2)$ is equal to the vibrational frequencies of a molecule. Peticolas et al.[33,34] used third-order time-dependent perturbation theory to calculate the Raman transition polarizabilities

$$\alpha_{gf,gi}^{\rho\sigma} = -\sum_{e,s}\left\{\frac{M_{ge}^{\rho} h_{es} M_{sg}^{\sigma}\langle f|Q|i\rangle}{[E_e^0 - E_g^0 + (f-i)\hbar\Omega - \hbar\omega_L][E_s^0 - E_g^0 - \hbar\omega_L]} + \text{c.c.}\right\} \quad (1)$$

where $M_{ge}^{\rho} \equiv \langle\phi_g^0|\mu_\rho|\phi_e^0\rangle$, $h_{es} \equiv \langle\phi_e^0|\partial H_E/\partial Q|\phi_s^0\rangle$, ϕ_g^0, ϕ_e^0, and ϕ_s^0 are the electronic ground and excited states at $Q = Q_0$ respectively, Q is the normal vibration coordinate, and $|i\rangle$ and $|f\rangle$ are initial and final vibration states in the ground electronic state. Because the sum over vibrational levels does not appear

in eq 1, this expression also contains a "trace" (e = s) B type term

$$A^{\rho\sigma}_{\mathrm{gf,gi}} = -\sum_{e}\left\{\frac{M^{\rho}_{\mathrm{ge}}h_{\mathrm{ee}}M^{\sigma}_{\mathrm{eg}}\langle f|Q|i\rangle}{[E^0_{\mathrm{e}}-E^0_{\mathrm{g}}-(\hbar\omega_{\mathrm{L}}-(f-i)\hbar\Omega)][E^0_{\mathrm{e}}-E^0_{\mathrm{g}}-\hbar\omega_{\mathrm{L}}]}+\mathrm{c.c.}\right\} \quad (2)$$

This term can be nonzero only for totally symmetric modes. From UV absorption spectra of BN in a 3 M NaOH aqueous solution (Figure 2), the incident photon energy $\hbar\omega_{\mathrm{L}}$ (λ_{ex}= 325 nm) is nearly resonant to the longest-wavelength absorption peak around 358 nm, and the scattered photon energy ($\hbar\omega_{\mathrm{L}} - (f - i)\hbar\Omega$) for the Ω= 1612 cm^{-1} mode is more near to the absorption peak, thus, on the basis of eq 2, $A^{\rho\sigma}_{\mathrm{gf,gi}}$ is approximate double-resonance enhancement. Also, eq 2 indicates that the 1612 cm^{-1} band is more favorably enhanced than that at 1366 cm^{-1}, because the scattering photon energy for the 1612 cm^{-1} band is closer the absorption peak. We can also use eq 1 to make similar and qualitative discussions on other B terms, because two excitation energy levels E^0_{e} and E^0_{s} of BN in an acetone solution result from the excitonic splitting of two degenerate levels and $\hbar(\omega_1 - \omega_2) = |E^0_{\mathrm{s}} - E^0_{\mathrm{e}}| = 0.22$ eV (1775 cm^{-1}),[14,19] which is approximately equal to the frequency of the 1612 cm^{-1} band and satisfies the above condition (ii). Here, we have assumed that for BN in basic solution $|E^0_{\mathrm{s}} - E^0_{\mathrm{e}}| \approx 0.22$ eV. The foregoing doubly resonant feature is worth studying further, because strong resonance enhancement, better assignment of modes through their selective resonance enhancement, and possible deduction of vibronic couplings for the modes are known to be the advantages of doubly resonant Raman spectroscopy.[14,32]

Second, on the basis of empirical observations of several molecules, Hirakawa and Tsuboi[35] formulated the called Tsuboi's rule: "If a Raman line becomes stronger when the exciting line is brought closer to the frequency of an electronic band $A \leftarrow X$, then the equilibrium conformation of the molecule is distorted along the normal coordinate for the Raman line in the transition from the ground state (X) to the excited state (A)." On the basis of a similar idea, Markham et al. made ab initio computation of the dimensionless displacement parameters and explained successfully the effect of deuterium substitution on RR spectra of imidazole and imidazolium.[22] The related electronic spectrum of BN results from the conjugated $\pi \rightarrow \pi^*$ transition of naphthol chromophore.[18,19] According to the foregoing theoretical investigations of the conjugate anionic bases of hydroxyaryls, the $S_0 \rightarrow S_1$ excitation of naphtholate and phenolate produces significant immigration of electron from the oxygen atom to the distal rings. This is expected to result in dramatic changes for the distances of the C_2-O_{11} bond. Our DFT calculation manifests that the 1612 cm^{-1} mode contains a significant contribution from the stretching of C_2-O_{11} bonds, thus according to Tsuboi rule, the 1612 cm^{-1} band is favorably resonance enhanced at the excitation λ_{ex}= 325 nm.

For further work, quantitative calculations of RR intensity are needed to account for the resonance enhancement without immediately resorting to the idea of double resonance enhancement. Resonance Raman intensities have been well-formulated either in a tranditional sum-over-state picture[39,34] or equivalently in the time-dependent resonance Raman formulas.[40,41] Although they are theoretically equivalent with each other, the time-dependent method has been proven to be more efficient in computation for systems with many vibrational modes. For the near-resonance case in this paper, more than one excited intermediate state contributes to the RR intensity and they have not clearly been identified now. Thus it is difficult to make a direct quantitative computation by using time-dependent method of RR scattering.[40−42] For "anomalous" deviations in the intensity pattern for individual bands such as the 1612 cm^{-1} band of BN^{2-}, after the simulation of RR spectra using the time-dependent RR method, additional resonance enhancement mechanisms might need to be analyzed by careful consideration of the feature of the energy denominator in RR formulas[42] as is done in this section.

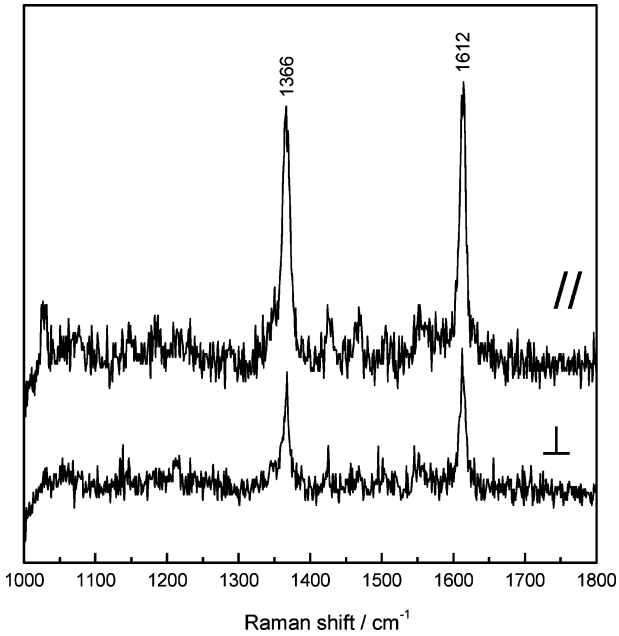

Figure 6. Polarized Raman spectrum of BN in a 3 M NaOH aqueous solution with the excitation wavelength λ_{ex}= 325 nm.

3.3.3. Polarization Properties of UVRR Spectra. The depolarization ratios of the 1366 and 1612 cm^{-1} bands in resonance Raman spectra of BN^{2-} at λ_{ex}= 325 nm were measured as 0.42 and 0.47 (see Figure 6), but 0.15 and 0.57 in normal Raman spectra at λ_{ex}= 514.5 nm (see Figure 4b), respectively.

The depolarization ρ describes the polarization properties and can be expressed by[20]

$$\rho = \frac{5\sum^1 + 3\sum^2}{10\sum^0 + 4\sum^2} = \frac{5(\sum^1/\sum^2) + 3}{10(\sum^0/\sum^2) + 4} \quad (3)$$

where Placzek invariants $\sum^0$, $\sum^2$, and $\sum^1$describe the isotropic, symmetric anisotropy, and antisymmetric part of the Raman tensors, respectively

$$\sum^0 = \frac{1}{3}|\alpha_{xx} + \alpha_{yy} + \alpha_{zz}|^2$$

$$\sum^1 = \frac{1}{2}\{|\alpha_{xy} - \alpha_{yx}|^2 + |\alpha_{xz} - \alpha_{zx}|^2 + |\alpha_{yz} - \alpha_{zy}|^2\}$$

$$\sum^2 = \frac{1}{2}\{|\alpha_{xy} + \alpha_{yx}|^2 + |\alpha_{xz} + \alpha_{zx}|^2 + |\alpha_{yz} + \alpha_{zy}|^2\} + \frac{1}{3}\{|\alpha_{xx} - \alpha_{yy}|^2 + |\alpha_{xx} - \alpha_{zz}|^2 + |\alpha_{yy} - \alpha_{zz}|^2\} \quad (4)$$

It is known[20] that in normal Raman spectra, antisymmetric transition polarizability or $\sum^1$ is zero, but in resonance Raman

scattering, Σ^1 can be nonzero. Thus, for the normal Raman spectra, the depolarization ratio ρ' is

$$\rho' = \frac{3}{4 + 10(\sum^0/\sum^2)} \tag{5}$$

and in resonance cases

$$\rho = \rho' + \frac{5(\sum^1/\sum^2)}{4 + 10(\sum^0/\sum^2)} \tag{3'}$$

$\rho = 0.42 > \rho' = 0.15$ for the 1366 cm^{-1} band of BN^{2-} and $\rho = 0.47 \approx \rho' = 0.57$ for the 1612 cm^{-1} band. Therefore, for the 1366 cm^{-1} band of BN^{2-}, not only the symmetric part contributes to this band but also the antisymmetric part; however, the 1612 cm^{-1} band does not include an antisymmetric Raman scattering contribution. The result for the 1366 cm^{-1} band of BN^{2-} agree with DR-SFV spectra of BN,[14,18] in which the 1377 cm^{-1} band of BN (corresponding to 1366 cm^{-1} of BN^{2-}) is most intensive and the strength of DR-SFVS from isotropic chiral liquids is proportional to the square of the corresponding antisymmetric Raman scattering tensor. But the 1612 cm^{-1} band is beyond the measured frequency region of DR-SFVS in ref 14 and needs to be further investigated by the DR-SFVS method.

For the 1366 cm^{-1} band of BN^{2-} in the normal Raman spectra, $\rho' = 0.15$, and so by use of eq 5

$$\sum^0/\sum^2 = 1.6 \tag{6}$$

Since in resonance cases $\rho = 0.42$, using eqs 3′, 6 and 5, we get

$$\sum^1/\sum^2 = 1.08 \tag{7}$$

From eqs 4 and 7, we can estimate the order of magnitude for the ratio K between antisymmetric (α_{anti}) and symmetric transition polarizabilities (α_{sym})

$$K = \frac{\alpha_{anti}}{\alpha_{sym}} \approx (\sum^1/\sum^2)^{(1/2)} = 1.04 \tag{8}$$

On the basis of the nonadiabatic correction terms of antisymmetric transition polarizability, Buckingham and Liu[36,37] gave the following formula of the order of magnitude of $\alpha_{anti}/\alpha_{sym}$

$$K' = \frac{\alpha_{anti}}{\alpha_{sym}} \approx \frac{\hbar\Omega}{E_e^0 - E_s^0} \tag{9}$$

where E_e^0 and E_s^0 are the energies of the excitation electronic states coupled by the mode $\hbar\Omega$, and Ω is the frequency of the vibration band. Here, for the 1366 cm^{-1} band, from the absorption spectra of BN in acetone solution,[19,14] the two peaks in the absorption spectrum come from transitions to the two exciton states separated by 0.22 eV, which corresponds to ($E_e^0 - E_s^0$) in the above equation,[14] thus

$$K' \approx \frac{1366}{0.22 \times 8065.7} = 0.77 \tag{10}$$

From eqs 8 and 10, the experiment and theory agree qualitatively with each other, which shows that the near-degeneracy of the excited-state levels (excitonic splittings) is important for the antisymmetric transition polarizability of BN.[37] In the nonresonance Raman scattering of tetrahydrofuran, analogous K' also appears in large-amplitude vibration modes of the ν_{16} and ν_{17} bands.[38] Other bands of BN^{2-} at 935, 1074, 1150, 1187, 1215, 1244, and 1287 cm^{-1} also have significant resonance enhancement, but are not clearly measured in the near-resonance polarized Raman spectrum of BN in a 3 M NaOH aqueous solution, Figure 6.

The present study for antisymmetric Raman scattering is qualitative and preliminary. To address the role of the antisymmetric Raman polarizability in doubly resonant SFG by the direct Raman spectroscopic study, we need further investigations in both experimental measurements and theoretical analysis. In experimental aspects (i) in general, if isotropic, symmetric, and antisymmetric scattering all contribute to a given Raman band, it is necessary to measure the reversal coefficient with circularly polarized light in 180° scattering in order to directly and quantitatively separate Σ^0, Σ^2, and Σ^1.[20] (ii) RR excitation profiles and depolarization dispersion curves for a given Raman band have been a central feature of experimental and theoretical work of RR spectra,[20] which is very important for investigations on antisymmetric Raman scattering because away from resonance, antisymmetric Raman tensors falls off much faster than symmetric ones because of the time-reversal symmetry arguments[37] or the interference effects from different vibronic transitions.[20] In theoretical aspects of RR spectra, quantitative calculations of RR intensity, depolarization ratios, and their dependence of the excitation frequencies are needed to account for the resonance enhancement. Finally, in addition to BN, more systems should be investigated by DR-SFVS and RR spectra.

4. Conclusions

We have measured the normal and UV near-resonance Raman (UVRR) spectra of 1,1′-bi-2-naphthol (BN) in basic solution. The polarized Raman scattering of BN in an acetone solution and BN in a 3 M NaOH aqueous solution were also studied. Density functional theory (DFT) calculations were carried out to study the vibrational frequencies and the ground-state structure of BN^{2-}. The assignments of observed Raman bands were proposed on the basis of the calculated and measured frequencies, intensities, and depolarization ratios. We analyzed the depolarization ratios of BN in basic solution at 1612 and 1366 cm^{-1} in normal Raman and UV resonance Raman spectra, which suggested that both the symmetric and the antisymmetric parts of Raman tensors contribute to the 1366 cm^{-1} band, but that only symmetric part contributes to the 1612 cm^{-1} band.

Acknowledgment. We are grateful to Professor A. D. Buckingham for very helpful comments on this paper. This work was supported by the National Natural Science Foundation of China (Grant 20473078, 20173051) and the Development Foundation of the Education Department of China (Grant 20020358061).

References and Notes

(1) Chen, Y.; Yekta, S.; Yudin, A. K. *Chem. Rev.* **2003**, *103*, 3155.
(2) Pu, L. *Chem. Rev.* **1998**, *98*, 2405.
(3) Shibasaki, M.; Sasai, H.; Arai, T. *Angew. Chem., Int. Ed.* **1997**, *36*, 1236.
(4) (a) Eilerts, N. W.; Heppert, J. A. *Polyhedron* **1995**, *14*, 3255. (b) Rosini, C.; Franzini, L.; Raffaelli, A.; Salvadori, P. *Synthesis* **1992**, 503.
(5) (a) Ishii, A.; Soloshonok, V. A.; Mikami, K. *J. Org. Chem.* **2000**, *65*, 1597. (b) Griffith, W. P.; Nogueira, H. I. S.; White, A. J. P.; Williams, D. J. *Polyhedron* **1997**, *16*, 1323. (c) Whitesell, J. K. *Chem. Rev.* **1989**, *89*, 1581. (d) Bringmann, G.; Walter, R.; Weirich, R. *Angew. Chem., Int. Ed.* **1990**, *29*, 977.
(6) (a) Kyba, E. P.; Gokel, G. W.; Jong, F. de; Koga, K.; Sousa, L. R.; Siegel, M. G.; Kaplan, L.; Sogah, G. D. Y.; Cram, D. J. *J. Org. Chem.*

1977, *42*, 4173. (b) Yudin, A. K.; Martyn, L. J. P.; Pandiaraju, S.; Zheng, J.; Lough, A. *Org. Lett.* **2000**, *2*, 41.

(7) Setnička, V.; Urbanová, M.; Bouř, P.; Král, V.; Volka, K. *J. Phys. Chem. A* **2001**, *105*, 8931.

(8) Sahnoun, R.; Koseki, S.; Fujimura, Y. *J. Mol. Struct.* **2005**, *735*−*736*, 315.

(9) Nogueira, H. I. S.; Quintal, S. M. O. *Spectrochim. Acta, Part A* **2000**, *56*, 959.

(10) Fischer, P.; Wiersma, D. S.; Righini, R.; Champagne, B.; Buckingham, A. D. *Phys. Rev. Lett.* **2000**, *85*, 4253.

(11) Belkin, M. A.; Kulakov, T. A.; Ernst, K.-H.; Yan, L.; Shen, Y. R. *Phys. Rev. Lett.* **2000**, *85*, 4474.

(12) (a) Belkin, M. A.; Han, S. H.; Wei, X.; Shen, Y. R. *Phys. Rev. Lett.* **2001**, *87*, 113001. (b) Ji, N.; Ostroverkhov, V.; Belkin, M. A.; Shiu, Y. J.; Shen, Y. R. *J. Am. Chem. Soc.* **2006**, *128*, 8845.

(13) Fischer, P.; Buckingham, A. D.; Albrecht, A. C. *Phys. Rev. A* **2001**, *64*, 053816.

(14) Belkin, M. A.; Shen, Y. R. *Phys. Rev. Lett.* **2003**, *91*, 213907.

(15) Fischer, P.; Wise, F. W.; Albrecht, A. C. *J. Phys. Chem. A* **2003**, *107*, 8232.

(16) (a) Buckingham, A. D.; Fischer, P. *Chem. Phys. Lett.* **1998**, *297*, 239. (b) Fischer, P.; Buckingham, A. D.; Beckwitt, K.; Wiersma, D. S.; Wise, F. W. *Phys. Rev. Lett.* **2003**, *91*, 173901.

(17) (a) Belkin, M. A.; Shen, Y. R. *Int. Rev. Phys. Chem.* **2005**, *24*, 257. (b) Fischer, P.; Hache, F. *Chirality* **2005**, *17*, 421.

(18) Zheng, R.-H.; Chen, D.-M.; Wei, W.-M.; He, T.-J.; Liu, F.-C. *J. Phys. Chem. B.* **2006**, *110*, 4480.

(19) Byers, J. D.; Hicks, J. M. *Chem. Phys. Lett.* **1994**, *231*, 216.

(20) Mortensen, O. S.; Hassing, S. *Adv. IR Raman Spectrosc.* **1980**, *6*, 1.

(21) (a) Becke, A. D. *J. Chem. Phys.* **1993**, *98*, 5648. (b) Lee, C.; Yang, W.; Parr, R. G. *Phys. Rev. B* **1988**, *37*, 785.

(22) Markham, L. M.; Mayne, L. C.; Hidson, B. S.; Zgierski, M. Z. *J. Phys. Chem.* **1993**, *97*, 10319.

(23) (a) Scott, A. P.; Radom, L. *J. Phys. Chem.* **1996**, *100*, 16502. (b) Oakes, R. E.; Spence, S. J.; Bell, S. E. J. *J. Phys. Chem. A* **2003**, *107*, 2964. (c) Xu, L.-C.; Li, Z.-Y.; Tan, W.; He, T.-J.; Liu, F.-C.; Chen, D.-M. *Spectrochim. Acta, Part A* **2005**, *62*, 850.

(24) Pasterny, K.; Wrzalik, R.; Kupka, T.; Pasterna, G. *J. Mol. Struct.* **2002**, *614*, 297.

(25) Devlin, F. J.; Stephens, P. J.; Österle, C.; Wiberg, K. B.; Cheeseman, J. R.; Frisch, M. J. *J. Org. Chem.* **2002**, *67*, 8090.

(26) Frisch, M. J.; Trucks, G. W.; Schlegel, H. B.; Scuseria, G. E.; Robb, M. A.; Cheeseman, J. R.; Montgomery, J. A., Jr.; Vreven, T.; Kudin, K. N.; Burant, J. C.; Millam, J. M.; Iyengar, S. S.; Tomasi, J.; Barnone, V.; Mennucci, B.; Cossi, M.; Scalmani, G.; Nega, N.; Petersson, G. A.; Nakatsuji, H.; Haha, M.; Ehara, M.; Toyota, K.; Fukuda, R.; Hasegawa, J.; Ishida, M.; Nakajima, T.; Honda, Y.; Kitao, O.; Nakai, H.; Klene, M.; Li, X.; Knox, J. E.; Hratchian, H. P.; Cross, J. B.; Adamo, C.; Jaramillo, J.; Gomperts, R.; Stratmann, R. E.; Yazyev, O.; Austin, J.; Cammi, R.; Pomelli, C.; Ochterski, J. W.; Ayala, P. Y.; Morokuma, K.; Voth, G. A.; Salvador, P.; Dannenberg, J. J.; Zakrzewski, V. G.; Dapprich, S.; Daniels, A. D.; Strain, M. C.; Farkas, O.; Malick, D. K.; Rabuck, A. D.; Raghavachari, K.; Foresman, J. B.; Ortiz, J. V.; Cui, Q.; Baboul, A. G.; Clifford, S.; Cioslowski, J.; Stefanov, B. B.; Liu, G.; Liashenko, A.; Piskorz, P.; Peng, C. Y.; Nanayakkara, A.; Challacombe, M.; Gill, P. M. W.; Johnson, B.; Chen, W.; Wong, M. W.; Gonzales, C.; Pople, J. A. *Gaussian 03*, revision B.03; Gaussian, Inc.: Pittsburgh, PA, 2003.

(27) Mori, K.; Masuda, Y.; Kashino, S. *Acta Crystallogr., Sect. C* **1993**, *49*, 1224.

(28) Agmon, N.; Rettig, W.; Groth, C. *J. Am. Chem. Soc.* **2002**, *124*, 1089.

(29) Granucci, G.; Hynes, J. T.; Millié, P.; Tran-Thi, T.-H. *J. Am. Chem. Soc.* **2000**, *122*, 12243.

(30) Scherer, J. R. *J. Chem. Phys.* **1962**, *36*, 3308.

(31) Didi, M. A.; Maki, A. K. T.; Mostafa, M. M. *Spectrochim. Acta, Part A* **1991**, *47*, 667.

(32) Ivchenko, E. L. *Optical Spectroscopy of Semiconductor Nanostructure*; Alpha Science: Harrow, UK, 2005; section 6.7.

(33) Peticolas, W. L.; Nafie, L.; Stein, P.; Fanconi, B. *J. Chem. Phys.* **1970**, *52*, 1576.

(34) Johnson, B. B.; Peticolas, W. L. *Annu. Rev. Phys. Chem.* **1976**, *27*, 465, eq. 25.

(35) Hirakawa, A. Y.; Tsuboi, M. *Science* **1975**, *188*, 359.

(36) Liu, F.-C. *J. Phys. Chem.* **1991**, *95*, 7180.

(37) Liu, F.-C.; Buckingham, A. D. *Chem. Phys. Lett.* **1993**, *207*, 325.

(38) Li, L.; He, T.-J.; Wang, X.-Y.; Zuo, J.; Xu, C.-Y.; Liu, F.-C. *Chem. Phys. Lett.* **1996**, *262*, 52.

(39) Tang, J.; Albrecht, A. C. In *Raman Spectroscopy*; Szymanski, H. A., Ed.; Plenum: New York, 1970; Vol. 2, Chapter 2.

(40) Lee, S.-Y.; Heller, E. J. *J. Chem. Phys.* **1979**, *71*, 4777.

(41) (a) Myers, A. B. *J. Raman Spectrosc.* **1997**, *28*, 389. (b) Leng, W.; Wurthner, F.; Kelley, A. M. *J. Phys. Chem. B* **2004**, *108*, 10284.

(42) Chen, D.-M.; He, T.-J.; Cong, D.-F.; Zhang, Y.-H.; Liu, F.-C. *J. Phys. Chem. A* **2001**, *105*, 3981.